Fitoterapia 140 (2020) 104440

Contents lists available at ScienceDirect

Fitoterapia

journal homepage: www.elsevier.com/locate/fitote

Anti-neuroinflammatory benzofurans and lignans from *Praxelis clematidea*

Lu Xiao[a], Yuying Huang[a], Yihai Wang[a,b,*], Jingwen Xu[a,b], Xiangjiu He[a,b,*]

[a] School of Pharmacy, Guangdong Pharmaceutical University, Guangzhou 510006, China
[b] Guangdong Engineering Research Center for Lead Compounds & Drug Discovery, Guangzhou 510006, China

ARTICLE INFO

Keywords:
Praxelis clematidea
Benzofurans
Lignans
Anti-neuroinflammatory
NO

ABSTRACT

Praxelis clematidea (Asteraceae) is a harmful invasive alien weed, which cause huge destruction of ecological environment and economic losses. In this study, 22 compounds were isolated and purified from the whole plant of *P. clematidea*, including 4 benzofurans (**1–4**), 18 lignans (**5–22**), and five of which were new compounds (**1**, **3**, **4**, **9**, **10**). Various spectroscopic analysis methods were utilized to elucidate their chemical structures. The inhibitory effects of the isolated compounds on NO release from BV-2 microglia cells induced by LPS were investigated. Most of the compounds showed pronounced anti-neuroinflammatory activity. Additionally, the new compounds **3**, **4** and **10** exhibited significant anti-neuroinflammatory effects, and the biological activities were further confirmed by immunoblotting, quantitative PCR and immunofluorescence staining assays. As results, this study provided a new idea for the further treatment and utilization of *P. clematidea* as anti-neuroinflammatory agents in health-benefit products.

1. Introduction

Praxelis clematidea (Griseb.) R. M. King & H. Robinson, also called praxelis, belongs to the genus *Eupatorium* in Compositae with unique bluish violet clusters of flowers and strong smell like cat urine after crushed. It is an annual to short-lived perennial herb [1]. The origin of praxelis is South America, and mainly distributes in Guangdong, Fujian, Hainan, Hong Kong and other tropical or subtropical coastal areas in China. Praxelis is extremely adaptable, and can grow in many climatic areas such as tropical, tropical rainforest, tropical grassland, subtropical and Mediterranean climate, etc. In recent years, it has rapidly invaded so many regions of the world, such as southern China, northern Queensland, Florida and so on. As an invasive harmful weed, praxelis often grows in woods, orchards, wasteland and shrubbery, etc. It consumes nutrients in the soil greatly and destroys the till ability of the soil because of its rapid reproductive capacity of growth base. Praxelis has a strong odor, which affects livestock forage and crop growth, and has a negative impact on agriculture, forestry and animal husbandry in many areas. It has become an invasive and malignant weed with destructive potential for local economic development [2,3]. Meanwhile, praxelis has allelopathy and repellency to other herbaceous plants in its invaded area, which posed a great threat to the survival and reproduction of other biological species, and resulted in a serious decline in the diversity and richness of local organisms [4].

It was found that praxelis was rich in flavonoids, terpenoids and steroids, among which polymethoxyflavones and sesquiterpenes had many biological activities [5]. The abundant flavonoids in praxelis were also found various biological activities, such as anti-inflammatory, antioxidant, anti-ulcer and anti-diarrheal [6]. Nevertheless, there are few reports about the chemical constituents of praxelis.

Inflammation is a protective response, involving immune cells, blood vessels and molecular mediators to protect against injury or infection [7]. Neuroinflammation belongs to an inflammation related to the nervous tissue. Chronic neuroinflammation is usually associated with neurodegenerative diseases, for instance, Alzheimer's disease (AD). Furthermore, the key mediators of the neuroinflammatory response in the brain are microglia, which are considered as the innate immune cells of central nervous system (CNS). Consequently, neuroinflammation induced by activation of microglia is supposed to be one of the prime reasons of AD [8].

In this study Recently, our research group has carried out a program to seeking anti-inflammatory lead compounds from high plants and a lot of bioactive natural products have achieved [9,10]. However, the alien invasive species praxelis had aroused our interest and concern. As a part of the program, we explored the biological activity of the chemical components isolated from praxelis, we found the notable anti-neuroinflammatory potential of these compounds, which is worth our further demonstrate and exploration. As a result, 22 compounds were isolated and identified, and their anti-neuroinflammatory activities were investigated as well.

* Corresponding authors.
E-mail addresses: wangyih88@163.com (Y. Wang), hexiangjiu@163.com (X. He).

https://doi.org/10.1016/j.fitote.2019.104440
Received 11 October 2019; Received in revised form 21 November 2019; Accepted 24 November 2019
Available online 26 November 2019
0367-326X/

2. Materials and methods

2.1. Instruments and reagents

Ultraviolet spectra (200–400 nm) were measured on a Pharmaspec UV-2550 UV–Vis spectrophotometer (Shimadzu, Kyoto, Japan). Infrared spectra were acquired by a Perkin Elmer 100 IR spectrometer (Waltham, MA, USA) with KBr pellets. Optical rotation experiments were carried out with an Autopol I polarimeter (Rudolph research analytical, Hackettstown, NJ, USA). The 1D and 2D NMR data were performed on a Bruker Avance III spectrometer (Falanden, Switzerland) using TMS as the internal standard. HR-ESI-MS data were recorded on a Waters Aquity UPLC-Q-TOF mass spectrometer (Milford, MA, USA). HPLC preparation were implemented by a semi-preparative HPLC with a 2535 pump and a 2489 UV–Vis detector (Milford, MA, USA), accompanied with a Cosmosil semi-preparative column ($5C_{18}$-MS-II, $5C_{18}$-AR-II, 10ID × 250 mm, Nacalai Tesque, Kyoto, Japan). Silica gel for open column chromatography (CC) was purchased from Anhui Liangchen silicon Source Material (Lu'an, China). ODS (40–60 μm, Merck KGaA, Darastadt, Germany) and Sephadex LH-20 (GE Healthcare Bio-Sciences, Pittsburgh, PA, USA) were used in purification.

All antibodies, antigens, enzymes were purchased from Cell Signaling Technology (Danvers, MA, USA). MTT was purchased from Sigma-Aldrich (St. Louis, MO, USA). Fluorescence microscope (Zeiss GmbH, Jena, Germany) was used for immunofluorescence imaging. The reverse transcription of RNA was promoted by PrimeScript RT Master Mix (TaKaRa, Beijing, China). Fluorescence quantification was realized by UltraSYBR Mixture (CWBIO, Beijing, China). Light Cycler 96 system (Roche Diagnostics, Mannheim, Germany) was used in the detection of PCR.

2.2. Plant materials

The whole plants of praxelis were collected from Guangzhou High Education Mega Center in August 2017. They were identified as *Praxelis clematidea* (Griseb.) R. M. King & H. Rob Robinson by Professor X. J. He of Guangdong Pharmaceutical University. The plant samples are kept in the Lead Compounds Laboratory of Guangdong Pharmaceutical University.

2.3. Extraction and isolation process

The air-dried whole plants of praxelis (10 kg) were crushed and extracted 4 times with 75% ethanol-water (4 × 80 L) at reflux. The solvent was condensed in vacuum and the ethanol-free suspension was successively extracted three times with the same volume of cyclohexane, chloroform, ethyl acetate and n-butanol, respectively.

The chloroform extract (74.68 g) was subjected to a silica gel column chromatography (CC) (200–300 mesh, 70 × 1230 mm) gradiently eluted with $CHCl_3$/MeOH system (100:1 to 1:1, *v*/v), and was divided into 19 fractions (PC-1 to 19). PC-5 (1.29 g) and PC-6 (1.32 g) were subjected to a silica gel CC eluted with cyclohexane/EtOAc (100:1 to 1:1, *v*/v), an ODS MPLC (MeOH/H_2O, 10:90 to 100:0, v/v), then used semi-preparative HPLC (MeOH/H_2O, 45/55, v/v) to afford compounds **16** (8.6 mg, t_R = 23.1 min) and **2** (4.3 mg, t_R = 24.3 min), respectively. Fraction PC-7 (877.1 mg) was applied to a silica gel CC (200–300 mesh, 25 × 340 mm) eluted gradiently with cyclohexane/acetone (50:1 to 1:1, *v*/v), by means of an ODS column (MeOH/H_2O, 10:90 to 80:20, v/v) and HPLC (MeOH/ H_2O, 40/60, v/v) to obtain compounds **13** (3.4 mg, t_R = 12.2 min) and **7** (10.8 mg, t_R = 32.5 min). PC-8 (3.66 g) was further subjected to a silica gel CC eluted gradiently with cyclohexane/acetone (30:1 to 1:1, *v*/v), an ODS MPLC (MeOH/H_2O, 20:80 to 90:10, v/v) and the semi-preparative HPLC (MeOH/H_2O, 40/60, *v*/v) to afford compound **8** (3.2 mg, t_R = 34.8 min). Fraction PC-9 (3.01 g) was divided into 11 subfractions (PC-9-1 to 11) by a silica gel CC (cyclohexane/EtOAc, 20:1 to 1:2, *v*/v). Compounds **5** (5.8 mg, t_R = 24.2 min) and **1** (5.0 mg, t_R = 39.6 min) were obtained from the fraction of PC-9-8 (1.42 g) by means of an ODS MPLC and the semi-preparative HPLC (MeOH/H_2O, 30/70, *v*/v). Subfraction PC-9-10 (368.8 mg) was purified by an ODS MPLC and the semi-preparative HPLC (MeOH/H_2O, 45/55, *v*/v) to acquire compound **10** (3.1 mg, t_R = 27.0 min) and used other mobile phase (MeOH/H_2O, 60/40, *v*/v) to afford compounds **3** (2.7 mg, t_R = 14.6 min) and **4** (3.3 mg, t_R = 16.3 min). Fraction PC-10 (4.49 g) was applied to a silica gel CC. gradiently eluted with cyclohexane/EtOAc (20:1 to 1:2, *v*/v) to obtain 13 subfractions (PC-10-1 to 13). Subfraction PC-10-10 (529.7 mg) was purified through an ODS MPLC and HPLC (MeOH/H_2O, 30/70, *v*/v) to acquire compound **14** (2.4 mg, t_R = 25.1 min), and compounds **12** (3.4 mg, t_R = 32.3 min), **6** (2.7 mg, t_R = 37.5 min) were obtained from MeOH/H_2O (45/55, *v*/v) as mobile phase. Subfraction PC-10-11 (879.3 mg) was further applied to an ODS MPLC and HPLC (MeOH/H_2O, 40/60, v/v) to get compounds **15** (13.9 mg, t_R = 13.2 min), **19** (13.9 mg, t_R = 25.5 min), **18** (5.8 mg, t_R = 27.7 min), **22** (7.1 mg, t_R = 35.1 min), **21** (6.9 mg, t_R = 38.1 min), **17** (5.4 mg, t_R = 44.4 min) and **20** (5.2 mg, t_R = 50.2 min), while compound **11** (6.4 mg, t_R = 28.7 min) was gotten from MeOH/H_2O (35/65, *v*/v) as mobile phase. Fraction PC-12 (5.21 g) was separated by a silica gel CC (cyclohexane/EtOAc, 20:0 to 1:0, v/v), ODS MPLC and HPLC (MeOH/H_2O, 45/55, v/v) to afford compound **9** (3.8 mg, t_R = 21.5 min).

Compound **1**, pale yellow amorphous powder, $[\alpha]^{25}{}_D$ + 3.0 (*c* 0.20, MeOH). CD (CH_3OH, $c = 1.3 \times 10^{-2}$ mol/L) λ_{max} ($\Delta\varepsilon$): 291 (−4.87), 226 (+4.26) nm. IR (KBr) ν_{max}: 3434, 2925, 1590, 1419, 1220, 1042 cm^{-1}. HR-ESI-MS *m/z* 251.0921 $[M + H]^+$ (calcd for $C_{13}H_{15}O_5$, 251.0919). ^1H NMR (DMSO-d_6, 600 MHz) and ^{13}C NMR (DMSO-d_6, 100 MHz) data, see Table 1.

Compound **3**, pale yellow amorphous powder, $[\alpha]^{25}{}_D$ + 46.2 (*c* 0.05, MeOH). CD (CH_3OH, $c = 5.5 \times 10^{-3}$ mol/L) λ_{max} ($\Delta\varepsilon$): 310 (+8.27), 280 (−0.30) nm. IR (KBr) ν_{max}: 3391, 2926, 1683, 1640, 1426, 1369, 1323, 1206, 1141, 803 cm^{-1}. HR-ESI-MS *m/z* 451.1385 $[M + H]^+$ (calcd for $C_{25}H_{23}O_8$, 451.1393). ^1H NMR (DMSO-d_6, 400 MHz) and ^{13}C NMR (DMSO-d_6, 100 MHz) data, see Table 1.

Compound **4**, pale yellow amorphous powder, $[\alpha]^{25}{}_D$ + 14.3 (*c* 0.05, MeOH). CD (CH_3OH, $c = 8.3 \times 10^{-3}$ mol/L) λ_{max} ($\Delta\varepsilon$): 310 (+11.69), 265 (−0.56) nm. IR (KBr) ν_{max}: 3429, 2925, 1643, 1430, 1371, 1325, 1207, 1138, 803 cm^{-1}. HR-ESI-MS *m/z* 451.1380 $[M + H]^+$ (calcd for $C_{25}H_{23}O_8$, 451.1393). ^1H NMR (DMSO-d_6, 400 MHz) and ^{13}C NMR (DMSO-d_6, 100 MHz) data, see Table 1.

Compound **9**, white amorphous powder, $[\alpha]^{25}{}_D$ − 82.3 (*c* 0.10, MeOH). CD (CH_3OH, $c = 8.45 \times 10^{-3}$ mol/L) λ_{max} ($\Delta\varepsilon$): 345 (+9.52), 215 (+23.50) nm. IR (KBr) ν_{max}: 3328, 2925, 1689, 1450, 1371, 1250, 1204, 1026 cm^{-1}. HR-ESI-MS *m/z* 413.1241 $[M-H]^-$ (calcd for $C_{22}H_{21}O_8$, 413.1242), ^1H NMR (acetone-d_6, 400 MHz) and ^{13}C NMR (acetone-d_6, 100 MHz) data, see Table 2.

Compound **10**, yellow amorphous powder, $[\alpha]^{25}{}_D$ + 9.2 (*c* 0.12, MeOH). CD (CH_3OH, $c = 3.0 \times 10^{-3}$ mol/L) λ_{max} ($\Delta\varepsilon$): 276 (+0.18), 238 (+0.54), 223 (−0.20) nm. IR (KBr) ν_{max}: 3407, 2924, 1684, 1508, 1465, 1208, 1132 cm^{-1}. HR-ESI-MS *m/z* 417.1552 $[M + H]^+$ (calcd for $C_{22}H_{25}O_8$, 417.1549). ^1H NMR (acetone-d_6, 500 MHz) and ^{13}C NMR (acetone-d_6, 125 MHz) data, see Table 2.

2.4. Anti-neuroinflammatory assay

BV-2 microglia cells were used to build up an in vitro neuroinflammation model. Cytotoxicity against BV-2 cells of the tested samples was measured by MTT assay and NO concentration was measured by Griess assay. The inhibitory effect of the samples on NO release from BV-2 cells was investigated. Meanwhile, the effects of the bioactive anti-neuroinflammatory compounds on proteins expression in BV-2 cells were analyzed by Western blot analysis, quantitative PCR and immunofluorescence assays.

Table 1
^{1}H and ^{13}C NMR data of compounds **1**, **3** and **4** isolated from *P. clematidea*[a].

No.	**1**		**3**		**4**	
	δ_H[b]	δ_C[c]	δ_H[c]	δ_C[c]	δ_H[c]	δ_C[c]
2		169.1		162.0		162.4
3	6.69 s	102.5		114.8		114.6
4	7.04 s	106.8	6.42 s	105.5	6.80 s	105.8
5		157.2		156.7		157.0
6		116.1		116.2		116.8
7	8.11 s	113.0	8.16 s	113.5	8.20 s	113.6
8		147.4		147.1		147.1
9		136.1		134.2		134.4
10		204.5		69.0		69.0
11	2.68 s	27.5	*α* 2.23 m; *β* 1.85 m	32.6	*β* 2.23 m; *α* 1.69 m	30.6
12		71.6	*a* 3.87 dd (10.5, 5.9); *b* 3.56 dd (10.5, 5.9)	65.9	*a* 3. 88 dd (10.6, 5.8); *b* 3.52 dd (10.6, 5.8)	65.7
13	3.60 d (10.8); 3.55 d (10.8)	68.2		204.4		204.5
14	1.44 s	23.6	2.67 s	27.6	2.70 s	27.6
2′				165.1		165.2
3′			6.76 s	103.9	6.36 s	103.8
4′			7.08 s	107.0	6.98 s	106.8
5′				157.4		157.3
6′				116.6		116.0
7′			8.11 s	113.1	8.10 s	113.0
8′				147.4		147.5
9′				135.9		136.0
10′			4.39 dd (8.3, 5.1)	33.4	4.50 dd (5.1, 3.0)	31.8
11′			*β* 2.28 m; *α* 2.20 m	25.7	*α* 2.38 m; *β* 2.16 m	24.0
12′				204.6		204.6
13′			2.65 s	27.4	2.68 s	27.4
5-OH			11.83 br. s		11.93 br. s	
10-OH			5.55 br. s		5.54 br. s	
12-OH			4.98 t (5.9)		4.94 t (5.8)	
5′-OH			12.02 br. s		11.99 br. s	

[a] Compounds **1**, **3** and **4** were measured in DMSO-d_6, δ in ppm and J in Hz;
[b] NMR spectra were acquired on an Avance III-600 NMR spectrometer;
[c] NMR spectra were acquired on an Avance III-400 NMR spectrometer.

2.4.1. LPS-induced NO production inhibitory assay

MTT assay was used to determine the inhibitory effect of the compounds on the proliferation of BV-2 microglia. In vitro anti-inflammatory activity was evaluated by measuring the concentration of NO in the medium according to the reported protocol [11]. BV-2 cells were inoculated into 96-well plates (2×10^5 cells/mL) and cultured at 37 ˚C for 24 h. Model group, blank group, negative control group and sample groups (the gradient dose concentration was 6.25, 12.5, 25, 50 μM, dissolved in DMSO) were set up, and 1 μg/mL LPS was added to continue incubation for 24 h. Collected 50 μL culture solution of each pore and mixed with 50 μL Griess A and Griess B reagents, respectively. Absorption was measured at 546 nm on a microplate reader, and the IC_{50} data was calculated by the Calcusyn software. Minocycline was used as positive control.

2.4.2. Immunoblot assay

The total protein of the cell was separated by electrophoresis and transferred from the gel to the membrane of solid support. And the antigen was detected by specific antibody, and the expression of iNOS and COX-2 was detected. The assay method was according to the previous literature [12]. Cells were inoculated on 12-well plate and added with samples of different concentration (12.5, 25, 50 μM), then treated with LPS (1 μg/mL), and incubated for 24 h. The total protein of monolayer adherent cells was extracted by lysis and centrifugation of cells. Western blot was performed with the extracted protein, and ECL kit was used to develop and image.

Table 2
^{1}H and ^{13}C NMR data of compounds **9** and **10** isolated from *P. clematidea*[a].

No.	**9**		**10**	
	δ_H[c]	δ_C[c]	δ_H[b]	δ_C[b]
1		123.9		128.0
2		129.9	6.83 s	106.4
3	6.62 s	116.1		148.8
4		144.7		137.4
5		147.2		148.8
6	6.95 s	115.9	6.83 s	106.4
7	7.55 s	137.2	4.96 d (8.0)	77.6
8		122.5	4.19 ddd (8.0, 4.3, 2.5)	79.3
9		166.3	3.74 dd (12.4, 2.5)	61.7
			3.52 dd (12.4, 4.3)	
10	4.14 m	60.3		
11	1.11 t (7.1)	13.5		
1′		135.2		127.8
2′	6.48 br. s	114.6	6.90 d (1.8)	111.2
3′		144.1		145.3
4′		144.6		137.0
5′	6.69 d (8.1)	115.0		150.4
6′	6.43 d (8.1)	118.8	6.98 d (1.8)	104.9
7′	4.42 d (3.1)	45.4	7.51 d (16.3)	143.9
8′	3.86 d (3.1)	47.7	6.69 d (16.3)	126.5
9′		171.9		197.8
10′	4.02 m	60.0	2.29 s	27.4
11′	1.24 t (7.1)	13.7		
3-OCH_3			3.85 s	56.8
5-OCH_3			3.85 s	56.8
5′-OCH_3			3.86 s	56.4

[a] Compounds **9** and **10** were measured in acetone-d_6, δ in ppm and J in Hz;
[b] NMR spectra were acquired on an Avance III-500 NMR spectrometer;
[c] NMR spectra were acquired on an Avance III-400 NMR spectrometer.

2.4.3. Quantitative RT-PCR analysis

BV-2 cells were pre-treated with samples and LPS (1 μg/mL), then incubated another 24 h. The control group (untreated culture medium), model group (treated with LPS) and sample group (treated with samples and LPS) were set up. Total RNA was purified using the AxyPrep Multisource RNA Miniprep Kit. The following primers were used: 5′-AGCCAAGCCCTCACCTACTT-3′ (F) and 5′-GCCTCCAATCTCTGCCTATC-3′ (R) for iNOS, 5′-TGAGTACCGCAAACGCTTCTC-3′ (F) and 5′-TGGACGAGGTTTTTCCACCAG-3′ (R) for COX-2, 5′-GTTGACGGACCCCAAAAGAT-3′ (F) and 5′-CCTCATCCTGGAAGGTCCAC-3 (R) for IL-1β. After the quantification of RNA, reverse transcription of RNA into cDNA and cDNA sequence amplification, then examination by PCR device, and the outcomes were processed and analyzed by LightCycler software version 1.1.0.1320. (Roche Applied Science, Mannheim, Germany).

2.4.4. Indirect immunofluorescence for NF-κB nuclear translocation

The Nuclear factor NF-κB pathway is a critical regulator of cellular response to stress and pathogens, and regulates the expression of genes involved in inflammatory response. BV-2 cells were seeded onto 48 well plates (3×10^4 cells/well), stimulated with LPS (1 μg/mL) and pre-treated with samples for 24 h, then fixed, permeabilized, blocked, and stained with NF-κB primary antibodies, Alexa Fluor 488 conjugated (1:500 dilutions) secondary antibody and Hoechst 33258 dye, sequentially. The untreated culture medium was used as blank control group, and the culture medium treated with 1 μg/mL LPS was set up as the model group. The Hoechst and Alexa Fluor fluorophores detected changes in nuclear morphology (blue fluorescence) and NF-κB distribution (green fluorescence), respectively. Fluorescence microscope was used for image acquisition and display.

2.5. Statistical analysis

All the experiments were carried out three times independently. Results were presented as the mean ± standard deviation (± SD). A

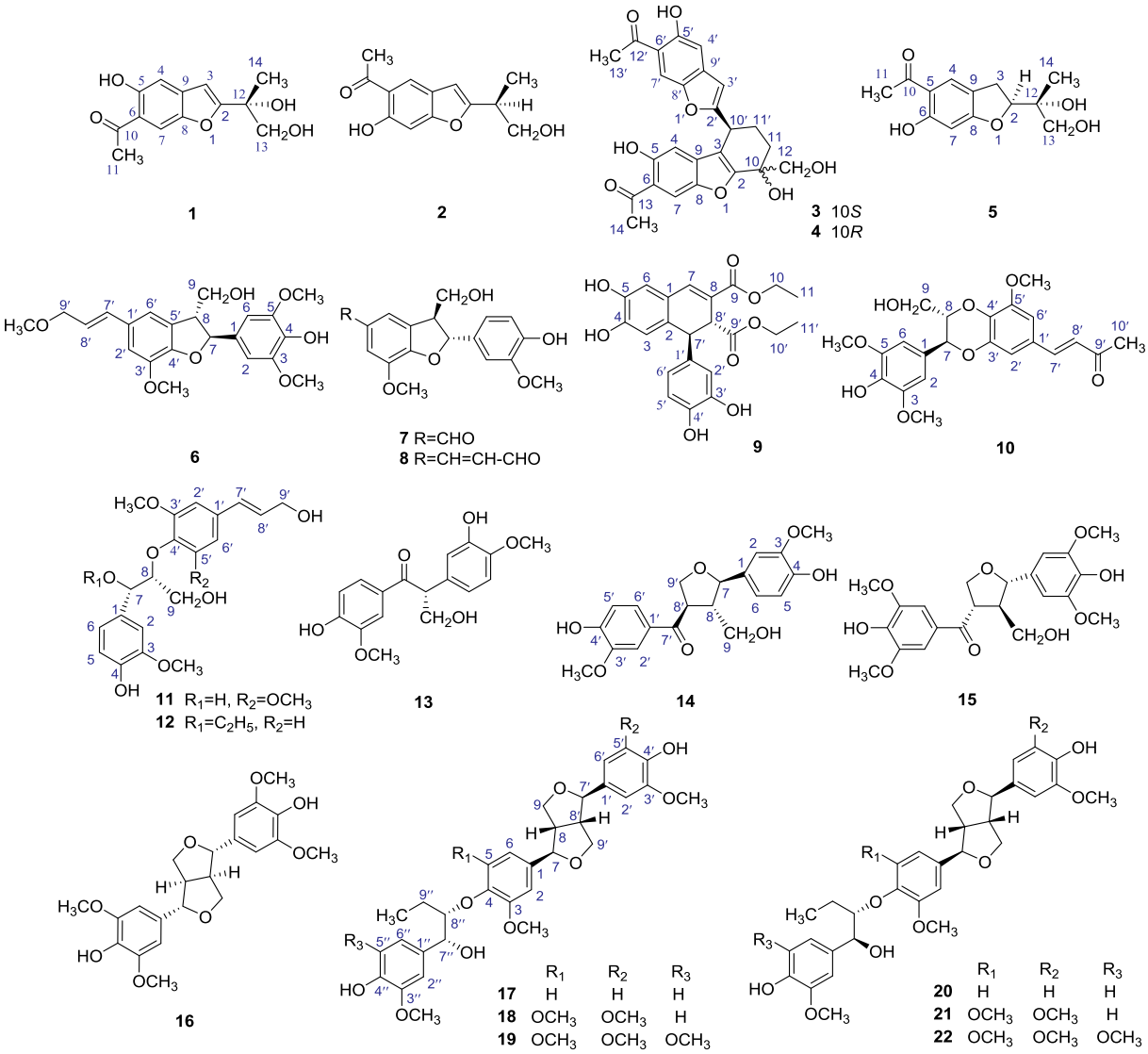

Fig. 1. Chemical structure of compounds **1–22** isolated from *P. clematidea*.

value of $p < 0.05$ was set for statistical significance.

3. Results and discussion

In this study, four benzofuran and eighteen lignans, including five new compounds (**1**, **3**, **4**, **9**, **10**), were isolated and identified from praxelis (Fig. 1). The anti-neuroinflammatory activities of all the compounds were evaluated, and most of them showed obvious biological activities.

3.1. Structural elucidation of the isolated compounds

Compound **1** was purified as pale yellow amorphous powder, $[\alpha]^{25}_{D}$ + 3.0 (*c* 0.20, MeOH). The molecular formula of $C_{13}H_{14}O_5$ was determined by the ion *m/z* 251.0921 $[M + H]^+$ (calcd for $C_{13}H_{15}O_5$, 251.0919) in its HR-ESI-MS (positive). In the ^{1}H NMR spectrum (Table 1), there were two sharp singlets at δ_H 8.11 (1H, s, H-7) and 7.04 (1H, s, H-4), elucidated as a tetra-substituted aromatic ring fragment with 1,2,4,5- substituted mode. Meanwhile, an olefinic signal at δ_H 6.69 (1H, s, H-3), two methylenes which coupled each other at δ_H 3.60 (1H, d, J = 10.8 Hz, H-13a) and 3.55 (1H, d, J = 10.8 Hz, H-13b), and two methyl signals at δ_H 2.68 (3H, s, H-11) and 1.44 (3H, s, H-14) were observed in the ^{1}H NMR. The ^{13}C NMR and DEPT spectra (Table 1) showed 13 carbons, including 2 × CH_3, 1 × CH_2, 3 × CH and 7 × C in the molecule. There were a ketone carbonyl at δ_C 204.5 (C-10), six aromatic carbons at δ_C 157.2 (C-5), 147.4 (C-8), 136.1 (C-9), 116.1 (C-6), 113.0 (C-7) and 106.8 (C-4), two olefinic carbons at δ_C 169.1 (C-2) and 102.5 (C-3), speculated that compound **1** possessed a benzofuran skeleton [13]. Moreover, the proton and carbon signals were assigned according to HSQC and HMBC experiments. The correlations from δ_H 2.68 (H−11) to δ_C 204.5 (C-10), 116.1 (C-6) and 113.0 (C-7), inferred that an acetyl group was linked to the aromatic ring at C-6. The correlations from δ_H 3.60 (H-13a) and 3.55 (H-13b) to δ_C 169.1 (C-2), 71.6 (C-12) and 23.6 (C-14), from δ_H 1.44 (H-14) to δ_C 169.1 (C-2), 71.6 (C-12) and 68.2 (C-13), indicated a unit of $C(CH_3)OHCH_2OH$ attached to C-2 of the skeleton. Compound **1** had a similar structure to gymnastone, and its NMR data were consistent with those reported [14]. The CD spectrum displayed a positive Cotton effect at 226 nm and a negative Cotton effect at 291 nm, hence, the configuration of compound **1** has been determined as *R* according to literature report [13]. Based on the above attributions, compound **1** was elucidated as (*R*)-5-hydroxy-6-acetyl-2-(1,2-hydroxy-1-methyl)benzofuran.

Compound **3** was obtained as a pale yellow amorphous powder, $[\alpha]^{25}_{D}$ + 46.2 (*c* 0.05, MeOH), which possessed the molecular formula of $C_{25}H_{22}O_8$ judged from the ion at *m/z* 451.1385 $[M + H]^+$ (calcd for $C_{25}H_{23}O_8$, 451.1393) in its HR-ESI-MS (positive). The ^{1}H NMR

spectrum (Table 1) of compound **3** showed the presence of two phenolic hydroxyls at δ_H 12.02 (1H, br. s, 5′-OH) and 11.83 (1H, br. s, 5-OH), four aromatic protons at δ_H 8.16 (1H, s, H-7), 8.11 (1H, s, H-7′), 7.08 (1H, s, H-4′) and 6.42(1H, s, H-4), one olefinic proton at δ_H 6.76 (1H, s, H-3′), two hydroxyls at δ_H 5.55 (1H, br. s, 10-OH) and 4.98 (1H, t, J = 5.9 Hz, 12-OH), two oxymethylenes at δ_H 3.87 (1H, dd, J = 10.5, 5.9 Hz, H-12a) and 3.52 (1H, dd, J = 10.5, 5.9 Hz, H-12b), four methylenes at δ_H 2.28 (1H, m, H-11′β), 2.23 (1H, m, H-11α), 2.20 (1H, m, H-11′α) and 1.85 (1H, m, H-11β), and two methyls at δ_H 2.67 (3H, s, H-14) and 2.65 (3H, s, H-13) in the molecule. The ^{13}C NMR and DEPT spectra (Table 1) revealed 25 carbons, including 2 × CH_3, 3 × CH_2, 6 × CH and 14 × C, which indicated that compound **3** was a benzofuran dimer [15]. The connection of each substituent can be determined by HMBC spectrum. The correlations from δ_H 5.55 (10-OH) to δ_C 162.0 (C-2), 69.0 (C-10), 65.9 (C-12) and 32.6 (C-11), from δ_H 4.39 (H-10′) to δ_C 165.1 (C-2′), 162.0 (C-2), 114.8 (C-3) and 25.7 (C-11′), suggested that the C-2 and C-3 of the benzofuran ring formed a six-member ring with C-10, 10′, 11 and 11′ bonds, as well as C-2′ of the other benzofuran unit linked to C-10′. Furthermore, the protons at δ_H 2.67 (H-14) had long range correlations with the carbons at δ_C 204.4 (C-13), 116.2 (C-6) and 113.5 (C-7), and the signal at δ_H 2.65 (C-13′) correlated with δ_C 204.6 (C-12′), 116.6 (C-6′) and 113.1 (C-7′), indicated that the C-6 and C-6′ of the two aromatic rings were linked an acetyl unit, respectively. Thus, the planar structure of compound **3** was determined from the above analysis. The NMR data of compound **3** were very similar to dieupachinin D isolated from *Eupatorium chinense* [15], the main difference was that compound **3** was lack a hydroxymethyl at C-10′. There were two chiral carbons located at C-10 and C-10′, and the relative configurations were determined by NOESY experiment. The correlations between H-3′ and H-11′β with H-11β, and between H-12a and H-11′α were revealed, indicating that H-10′ and 10-OH were on the opposite side. The CD spectrum showed a negative Cotton effect at 280 nm and a positive Cotton effects at 310 nm, and the absolute configuration was selected for conformational analysis and ECD calculations. Therefore, the absolute configuration of **3** was established to be 10*S*,10′*S* [15] (Fig. 2). Based on above analysis, compound **3** was elucidated to be (+)-1-{2-[(1*S*,4*S*)-7-acetyl-4,8-dihydroxy-4-hydroxymethyl-1,2,3,4-tetrahydrodibenzo[b,d]-furan-1-yl]-5-hydroxy-1-benzofura −6-yl}ethanone.

Compound **4** was isolated as a pale yellow amorphous powder, $[\alpha]^{25}_D$ + 14.3 (*c* 0.05, MeOH), which had a same molecular formula of $C_{25}H_{22}O_8$ as compound **3** according to the quasi-molecular ion peak at *m/z* 451.1380 $[M + H]^+$ (calcd for $C_{25}H_{23}O_8$, 451.1393) in HR-ESI-MS (positive). Comparison of ^{1}H and ^{13}C NMR spectra data of compound **3** with those of compound **4**, displayed that their NMR signals were similar. In the ^{1}H NMR spectrum of **4** (Table 1), four methylene signals at δ_H 2.38 (1H, m, H-11′α), 2.23 (1H, m, H-11β), 2.16 (1H, m, H-11′β) and 1.69 (1H, m, H-11α), as well as the coupling constants of the proton at δ_H 4.50 (1H, dd, J = 5.1, 3.0 Hz, H-10′) were slightly different from those of **3**. In the ^{13}C NMR spectrum (Table 1), meanwhile, the methine at δ_C 31.8 (C-10′) and two methylenes at δ_C 30.6 (C-11) and 24.0 (C-11′) had some differences in chemical shifts compared with **3**. Based on the data of the ^{1}H–^{1}H COSY, HSQC and HMBC, it speculated that the compounds **3** and **4** had same planer structure, while the configuration of C-10 changed. Observed from the NOESY spectrum, between H-3′ and H-11′β with H-11β, between H-10′ and H-11α, between H-12a/H-12b and H-11′β had NOE effects, suggested that 10-OH was on the same side as H-10′ [15]. Additionally, the CD spectrum of compound **4** was similar to that of **3**, the negative Cotton effect at 265 nm and a positive Cotton effects 310 nm were indicated in the CD spectrum. According to the ECD calculations, the absolute configuration of **4** was inferred to be 10*R*,10′*S* (Fig. 2). As a result, compound **4** was established as (+)-1-{2-[(1*R*,4*S*)-7-acetyl-4,8-dihydroxy-4-hydroxymethyl-1,2,3,4-tetrahydrodibenzo[b,d] furan-1-yl]-5-hydroxy-1-benzofuran-6-yl}ethanone.

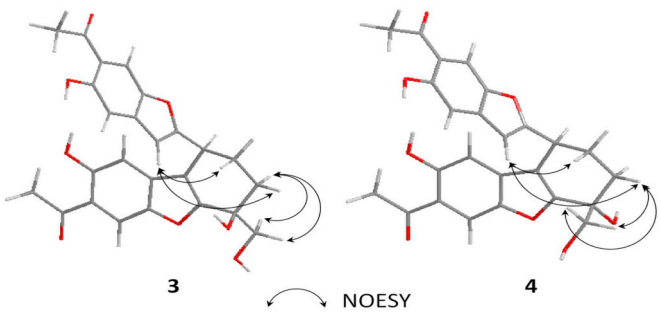

Fig. 2. Key NOE correlations of compounds **3** and **4.**

Compound **9** was existed as white amorphous powder, $[\alpha]^{25}_D$ − 82.3 (*c* 0.10, MeOH). The molecular formula of $C_{22}H_{22}O_8$ was deduced according to the quasi-molecular ion peak *m/z* 413.1241 $[M-H]^-$ (calcd for $C_{22}H_{21}O_8$, 413.1242) in its HR-ESI-MS (negative). In the ^{1}H NMR spectrum (Table 2), a benzene ring fragment of ABX spin system could be inferred from δ_H 6.69 (1H, d, J = 8.1 Hz, H-5′), 6.48 (1H, br. s, H-2′) and 6.43 (1H, d, J = 8.1 Hz, H-6′) in the aromatic region. The two single peaks at δ_H 6.95 (1H, s, H-6) and 6.62 (1H, s, H-3) inferred to an aromatic ring with 1,2,4,5-substitution mode, and a sharp singlet at δ_H 7.55 (1H, s, H-7) was presumed to a proton signal on the double bond. Signals at δ_H 4.42 (1H, d, J = 3.1 Hz, H-7′) and 3.86 (1H, d, J = 3.1 Hz, H-8′), which coupled each other, inferred two proton signals of adjacent methines. Protons at δ_H 4.14 (2H, m, H-10) and 4.02 (2H, m, H-10′) were two oxymethylenes, and the signals at δ_H 1.24 (3H, d, J = 7.1 Hz, H-11′) and 1.11 (3H, d, J = 7.1 Hz, H-11) were two methyls. The ^{13}C NMR and DEPT spectra (Table 2) had a total of 22 carbons, which contained 2 methyls, 2 methylenes, 8 methines and 10 quaternary carbons. Based on the above description, the skeleton of compound **9** was a 2,7′-cyclolignan [16]. The HMQC and HMBC spectra were used to assign the signals. In the HMBC spectrum, the correlations from δ_H 7.55 (H-7) to δ_C 129.9 (C-2), 123.9 (C-1), 47.7 (C-8′), from δ_H 4.42 (H-7′) to δ_C 135.2 (C-1′), 129.9 (C-2), 122.5 (C-8), and from δ_H 3.86 (H-8′) to δ_C 137.2 (C-7), 129.9 (C-2), 122.5 (C-8), 45.4 (C-7′), speculated that C-8 with C-8′ and C-2 with C-7′ were connected to formed a six-membered ring between the two C_6C_3 units. The correlations from δ_H 4.14 (*H*−10) to δ_C 166.3 (C-9), 13.5 (C-11), from δ_H 4.02 (H-10′) to δ_C 171.9 (C-9′), 13.7 (C-11′), from δ_H 1.24 (H-11′) to δ_C 60.0 (C-10′), and from δ_H 1.11 (H-11) to δ_C 60.3 (C-10) confirmed that compound **9** existed the diethyl esters [17]. According to the coupling constant of H-7′ and H-8′ ($J_{7',8'}$ = 3.1 Hz), the configuration of compound **9** was deduced to be *trans* [16]. By CD experiment, a positive Cotton effect was observed at 345 nm, and the calculated ECD data of **9** were similar to its methyl ester derivative 4a published in Tetrahedron [18]. Therefore, the absolute configurations was determined to be 7′*S*,8′*R*. Based on above analysis, compound **9** was identified as (7′*S*,8′*R*)-4,5,3′,4′-tetrahydroxy-2,7′- cyclolign-7-ene-9,9′-dioic acid diethyl ester.

Compound **10** was obtained as yellow amorphous powder, $[\alpha]^{25}_D$ + 9.2 (*c* 0.12, MeOH). The molecular formula was determined to $C_{22}H_{24}O_8$ according to the ion *m/z* 417.1552 $[M + H]^+$ (calcd for $C_{22}H_{25}O_8$, 417.1549) in the HR-ESI-MS (positive). The ^{1}H NMR spectrum (Table 2) of **10** exhibited two tetra-substituted aromatic rings, one of them at δ_H 6.98 (1H, d, J = 1.8 Hz, H-6′) and 6.90 (1H, d, J = 1.8 Hz, H-2′), and the other with two equivalent aromatic protons at δ_H 6.83 (2H, s, H-2 and 6). Two olefinic protons at δ_H 7.51 (1H, d, J = 16.3 Hz, H-7′) and 6.96 (1H, d, J = 16.3 Hz, H-8′) existed on a *trans* carbon-carbon double bond. A three-carbon sequence, CH(O)CH(O)CH_2OH, inferred from δ_H 4.96 (1H, d, J = 8.0 Hz, H-7), 4.19 (1H, ddd, J = 8.0, 4.3, 2.5 Hz, H-8), δ_H 3.74 (1H, dd, J = 12.4, 2.5 Hz, H-9a) and 3.52 (1H, dd, J = 12.4, 4.3 Hz, H-9b), and a fragment of benzo-1,4-dioxane was formed. It was also revealed that three methoxyl groups at δ_H 3.86 (3H, s, 5'-OCH_3), 3.85 (6H, s, 3 and 5-OCH_3), and one methyl at

Table 3
Inhibitory effects on NO production induced by LPS in BV-2 cells of the compounds from *P. clematidea*.

Compound	IC_{50} (μM)[a]	Cell viability	Compound	IC_{50} (μM)[a]	Cell viability
1	79.97 ± 10.05	> 100	**13**	69.36 ± 6.23	> 100
2	25.39 ± 2.21	> 100	**14**	95.31 ± 0.35	> 100
3	19.30 ± 1.43	> 100	**15**	70.40 ± 4.51	> 100
4	11.62 ± 3.42	> 100	**16**	39.36 ± 3.71	> 100
5	94.39 ± 3.75	> 100	**17**	17.76 ± 4.34	> 100
6	15.19 ± 4.56	> 100	**18**	27.94 ± 4.28	> 100
7	63.70 ± 0.61	> 100	**19**	47.79 ± 3.71	> 100
8	15.14 ± 2.77	> 100	**20**	16.81 ± 2.01	> 100
9	70.70 ± 3.58	> 100	**21**	66.94 ± 5.65	> 100
10	27.54 ± 8.08	> 100	**22**	40.71 ± 15.19	> 100
11	26.74 ± 6.97	> 100	**Minocycline**[b]	23.15 ± 1.04	> 100
12	16.25 ± 3.74	58.05 ± 18.66			

[a] Values were presented as means ± SD (n = 3);
[b] Positive control.

δ_H 2.29 (3H, s, H-10′) in ^{1}H NMR. The ^{13}C NMR and DEPT showed 22 carbons (Table 2), which ascribed to 15 olefinic (6 × CH and 9 × C) and 7 aliphatic (4 × CH_3, 1 × CH_2, 2 × CH) carbons. Combining with the ^{1}H NMR, it was inferred that the skeleton of compound **10** were 3′,7-epoxy-8,4′-oxyneolignans. The HMBC and ^{1}H−^{1}H COSY spectra indicated the correlations of δ_H 2.29 (H-10′) with δ_C 197.8 (C-9′) and 126.5 (C-8′), and δ_H 7.51 (H-7′) with δ_C 197.8 (C-9′), 127.8 (C-1′), 126.5 (C-8′), 111.2 (C-2′), which could be verified that the acetyl group was linked to the 3-methoxy-4,5-dioxophenyl group through a double bond. The three-carbon sequence, CH(O)CH(O)CH_2OH, was link to the other symmetrical aromatic ring at δ_C 128.0 (C-1) supported by long range correlations of δ_H 4.96 (H-7) with δ_C 106.4 (C-2 and C-6), 79.3 (C-8) and 61.7 (C-9). Furthermore, the stereochemistry between H-7 and H-8 led to the coupling constant about $J_{7,8}$ = 8.0 Hz, the NOE correlations between H-8/H-6 and H-7/H-9 clearly indicated the relative configuration was determined as *threo* [19]. The absolute configuration of **10** was 7*S*,8*S* indicated by CD spectrum with two positive Cotton effects at 276 and 238 nm, and a negative Cotton effect at 223 nm [20]. Therefore, compound **10** was identified as 4-[(3*S*)-(4-hydroxy-3,5-dimethoxyphenyl)-(2*S*)-hydroxymethyl-8-methoxy-2,3-dihydrobenzo-[1,4]dioxin-6-yl]-(3*E*)-buten-2-one.

The remaining 17 known compounds were identified as (*S*)-11-hydroxy- 10,11-dihydro-euparin (**2**) [21], (−)-1-[2-(1,2-dihydroxy-1-methylethyl)-2,3-dihydro- 6-hydroxy-5-benzofuranyl-ethanone (**5**) [22], (−)-(7*R*,8*S*, 7′*E*)-4-hydroxy-3,5,5′,9′- tetramethoxy-4′,7-epoxy-8,3′-neolign-7′-en-9-ol (**6**) [23], (+)-ficusal (**7**) [24], (+)-balanophonin (**8**) [25], (+)-*erythro*-syringylglycerol-β- O-4′-sinapyl ether (**11**) [26], (+)-xanthiumnolic A (**12**) [27], (−)-evofolin B (**13**) [28], (+)-(7′*R*,8*R*,8′*S*)-4,4′,9′- trihydroxy-3,3′-dimethoxy-7′,9-epoxylignan-7-one (**14**) [29], (−)-(7′*S*,8*S*,8′*R*)-4,4′- dihydroxy-3,3′,5,5′-tetramethoxy-7′,9-epoxylignan-9′-ol-7-one. (**15**) [30], (−)-syringaresinol (**16**) [31], (−)-(7*R*,7′*R*,7″*R*,8*S*,8′*S*,8″*S*)-4′,4″-dihydroxy-3,3′,3″-trimethyl-pentameth-oxy-7,9,7′,9′-diepoxy-4,8″-oxy-8,8′-sesquineolignan-7″,9″-diol (**17**) [32,33], (−)-(7*R*,7′*R*,7″*R*,8*S*,8′*S*,8″*S*)-4′,4″-dihydroxy-3,3′,3″,5,5′-pentameth- oxy-7,9,7′,9′-diepoxy-4,8″-oxy-8,8′-sesquineolignan-7″,9″-diol (**18**) [30], (+)-(7*R*,7′*R*, 7″*R*,8*S*,8′*S*,8″*S*)-4′,4″-dihydroxy-3,3′,3″,5,5′,5″-hexamethoxy-7,9,7′,9′-diepoxy-4,8″- oxy-8,8′-sesquineolignan-7″,9″-diol (**19**) [34], (−)-(7*R*,7′*R*,7″*S*,8*S*,8′*S*,8″*S*)-4′,4″- dihydroxy-3,3′,3″-trimethyl-pentameth-oxy-7,9,7′,9′-diepoxy-4,8″-oxy-8,8′-sesquineolignan-7″,9″-diol (**20**) [32,33], (−)-(7*R*,7′*R*,7″*S*,8*S*,8′*S*,8″*S*)-4′,4″-dihydroxy-3,3′,3″,5,5′- pentameth-oxy-7,9,7′,9′-diepoxy-4,8″-oxy-8,8′-sesquineolignan-7″,9″-diol (**21**) [34], and (−)-(7*R*,7′*R*,7″*S*,8*S*,8′*S*,8″*S*)-4′,4″-dihydroxy-3,3′,3″,5,5′,5″-hexa-methoxy- 7,9,7′,9′-diepoxy-4,8″-oxy-8,8′-sesquineolignan-7″,9″-diol (**22**) [35], respectively, based on their spectroscopic data compared with those reported in the literature.

3.2. Anti-neuroinflammatory activities

NO production was considered as an important factor lead to inflammation. The anti-neuroinflammatory activities of all isolated compounds were summarized in Table 3. The viability of BV-2 microglia cells was determined by MTT assay. The results showed that the 22 compounds except compound **12** performed no obvious cytotoxicity to BV-2 cells at the maximum concentrations of 100 μM, indicated that the NO inhibitory effects of the tested compounds was not caused by cytotoxicity. In LPS-induced NO production inhibitory assay, most of the compounds have anti-neuroinflammatory activity. Compounds **3**, **4**, **6**, **8**, **12**, **17** and **20** were displayed significant anti-neuroinflammatory activity (IC_{50} < 20 μM) compared to minocycline (IC_{50} = 23.15 ± 1.04 μM). Among them, compound **4**, a benzofuran dimer, had the most significant activity with the IC_{50} value of 11.62 ± 3.42 μM. Besides, compounds **2**, **10**, **11**, **16**, **18**, **19** and **22** indicated obvious anti-neuroinflammatory activities (IC_{50} = 20 to 50 μM). According to the bioactivity results, the C_6C_3 unit in the structure did not seem to be a key factor to inhibit the production of NO, while substituent group on the skeleton or configuration of the structure acted an important role.

The new compounds **3**, **4** and **10** had obvious anti-inflammatory activities and their effects on the accumulation of pro-inflammatory factors iNOS and COX-2 in LPS-stimulated BV-2 cells were analyzed by Western blot. As shown in Fig. 3A and Fig. 3B, the LPS group showed an obvious upward trend compared with the model group. Compounds **3**, **4** and **10** were found to be dose-dependently reducing the LPS-induced iNOS expressions, and had no obvious effects in COX-2 expressions, which revealed that the NO inhibitory effect of the compounds may be exerted via iNOS related pathway. In addition, the effects of the compounds on the mRNA levels in LPS-activated BV2 cells were also examined by PCR assay. In Fig. 3C, the mRNA levels of iNOS, COX-2, IL-1β were noticeably increased after LPS (1 μg/mL) stimulation. Compounds **3** and **4** pre-treatment dose-dependently inhibited the expressions of iNOS and IL-1β mRNA in LPS-induced BV-2 cells. Nevertheless, the inhibitory effects of the three compounds on COX-2 mRNA level were not significantly at the same condition, except compound **4**. The results demonstrated that the compounds certainly inhibited the NO production, the expression of iNOS, COX-2 and pro-inflammatory cytokine IL-1β in LPS-stimulated BV-2 cells.

Using immunofluorescent staining of BV-2 cells challenged with LPS, it found that compounds **3**, **4** and **10** were capable of blocking NF-κB translocation from cytoplasmic to nuclear. By observing by microscopy in living cells, it was discovered that the NF-κB in LPS-stimulated BV-2 cells aggregated to the nucleus in large quantities compared with the control group. However, the nuclear translocation and accumulation of NF-κB diminished owing to compounds pretreatment (Fig. 4). All

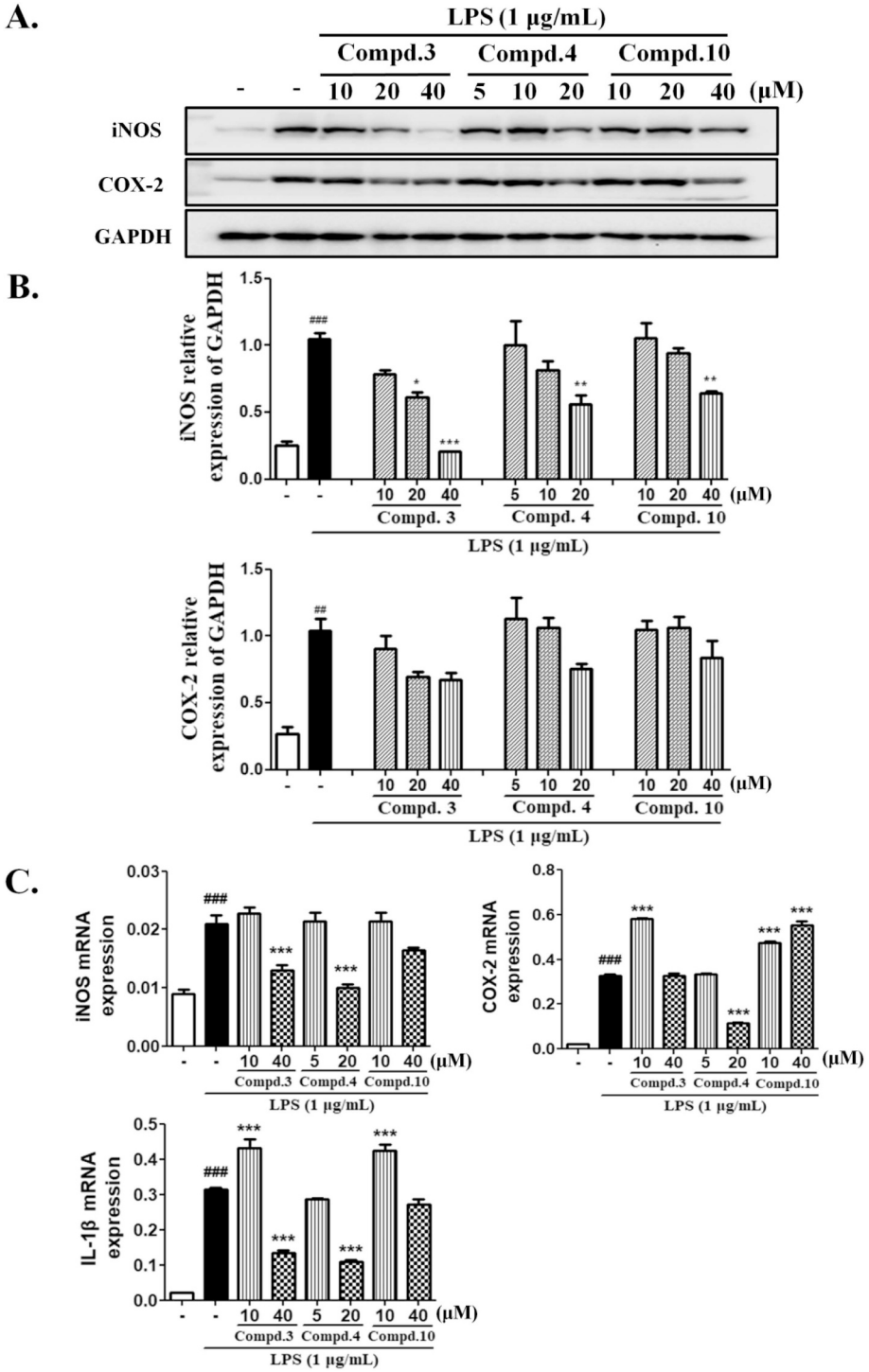

Fig. 3. Inhibitory effects on the expression levels of pro-inflammatory mediators of iNOS, COX-2 and IL-1β in LPS-stimulated BV-2 cells of compounds **3**, **4** and **10**.
A. Immunoblotting results of the LPS-stimulated iNOS and COX-2 protein expression in LPS-stimulated BV-2 cells.
B. The quantitative analysis of the expression of iNOS and COX-2 in BV-2 cells by immunoblotting.
C. The quantitative analysis of iNOS, COX-2 and IL-1β mRNA levels in LPS-stimulated BV-2 cells by RT-PCR.
$^{\#\#}p < 0.01$, $^{\#\#\#}p < 0.001$ vs. control group, $^{*}p < 0.05$, $^{**}p < 0.01$, $^{***}p < 0.001$ vs LPS group.

the above indicated that compounds isolated from praxelis have great potentiality of anti-neuroinflammatory.

4. Conclusion

In this paper, 3 new benzofurans, 2 new lignans and 17 known compounds were purified and identified from praxelis. The anti-neuroinflammatory activities of the isolated compounds were evaluated by LPS-induced NO production in microglia BV-2 cells, and the results exhibited that the majority of them displayed potent anti-neuroinflammatory activity. Meanwhile, immunoblotting, immunofluorescence assay and quantitative RT-PCR were used to further verify the anti-inflammatory activity of the isolated compounds from cell and mRNA expression levels. These results indicated that the compounds obtained

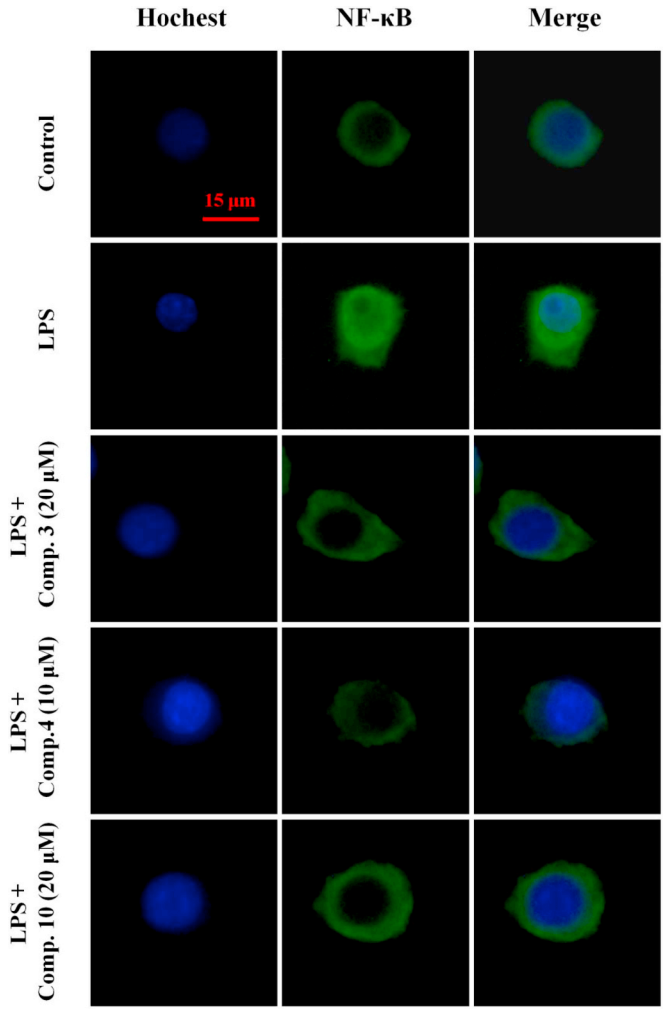

Fig. 4. Compounds **3**, **4** and **10** inhibited NF-κB nuclear translocation in BV-2 cells.
The transcription factor, NF-κB, was stained with Primary antibodies NF-κB followed by Alexa Fluor 488 conjugated secondary antibody (green fluorescence) and Hoechst 33258 dye (blue fluorescence), sequentially. (For interpretation of the references to colour in this figure legend, the reader is referred to the web version of this article.)

from praxelis exhibited potent anti-neuroinflammatory activity.

This study indicated that praxelis was considered as a harmful weed to be removed and rejected, but it could be used as a cheap source of anti-neuroinflammatory compounds. Therefore, the rational management of praxelis is not only become beneficial resources to improve the ecological environment, but also has great significance for finding bioactive substances that can be used in medicine, cosmetics and agricultural industry.

Declaration of Competing Interest

The author states that there is no conflict of interest in this article.

Acknowledgments

This work was funded by Guangdong Province Universities and Colleges Pearl River Scholar Funded Scheme (2017) and the Pearl River S&T Nova Program of Guangzhou (201806010169).

Appendix A. Supplementary data

Supplementary data to this article can be found online at https://doi.org/10.1016/j.fitote.2019.104440.

References

[1] J.R. Abbott, C.L. White, S.B. Davis, *Praxelis clematidea* (Asteraceae), a genus and species new for the flora of North America, J. Bot. Res. Inst. Tex. 2 (2008) 621–626.
[2] Q. Wang, H. Min, S.R. Downie, Z. Chen, Y. Chen, Genetic diversity and structure of the noxious alien grass *Praxelis clematidea* in southern China, Biochem. Syst. Eco. 59 (2015) 183–189.
[3] K.A. Shaw, J.C. Kernot, Extent of dense native woodland and exotic weed infestation in the extensive grazing lands of the Upper Herbert and Upper Burdekin River Catchments of far North Queensland: results of a producer survey, Trop. Grasslands 38 (2004) 112–116.
[4] X.R. Huang, S.L. Pang, W.H. Shen, Y.R. Hou, F. He, Herb diversity and its affecting factors of community invaded by *Praxelis clematidea* in karst mountainous area of Guangxi Province, China, Chin. J. Appl. Ecol. 27 (2016) 815–821.
[5] N. Wang, L. Tang, X. Yang, S. Deng, Chemical constituents of *Eupatorium catarium* as an alien invasive plant, Pratac. sci. 28 (2011) 1882–1887.
[6] E. Middleton, C. Kandaswami, T.C. Theoharides, The effects of plant flavonoids on mammalian cells: implications for inflammation, heart disease, and cancer, Pharmacol. Rev. 52 (2000) 673–751.
[7] T.J. Guzik, R. Korbut, T. Adamekguzik, Nitric oxide and superoxide in inflammation and immune regulation, J. Physiol. Pharmacol. 54 (2003) 469–487.
[8] T. Wyss-Coray, Ageing, neurodegeneration and brain rejuvenation, Nature 539 (2016) 180–186.
[9] L.M. Xiang, X.M. Yi, Y.H. Wang, X.J. He, Steroidal alkaloid glycosides and phenolics from the immature fruits of *Solanum nigrum*, Fitoterapia 137 (2019) 104268.
[10] F. Yan, Y.Y. Huang, Y.H. Wang, Q. Li, X.J. He, Bioactive sterols and triterpenoids from the fruits of giant crepe-myrtle, Ind. Crop. Prod. 130 (2019) 363–370.
[11] Y.H. Wang, L.M. Xiang, X.M. Yi, X.J. He, Potential anti-inflammatory steroidal saponins from the berries of *Solanum nigrum* L. (European Black Nightshade), J. Agric. Food Chem. 65 (2017) 4262–4272.
[12] X.M. Yi, L.M. Xiang, Y.Y. Huang, Y.H. Wang, X.J. He, Apoptosis and pro-death autophagy induced by a spirostanol saponin isolated from *Rohdea chinensis* (Baker) N. Tanaka (synonym *Tupistra chinensis* Baker) on HL-60 cells, Phytomedicine 42 (2018) 83–89.
[13] X.S. Zhang, J.Q. Cao, Z.T. Liu, Y. Lei, C. Gang, J.X. Liu, F.Z. Qu, Y.Q. Zhao, Callistephus A, a novel sesquiterpene from the *Callistephus chinensis* flower, Phytochem. Lett. 11 (2014) 5–8.
[14] N.T. Dat, P. Kiem, F.X. Van Cai, Q. Shen, K. Bae, Y.H. Kim, Gymnastone, a new benzofuran derivative from *Gymnaster koraiensis*, Arch. Pharm. Res. 27 (2004) 1106–1108.
[15] W.J. Wang, L. Wang, Z. Liu, R.W. Jiang, Z.W. Liu, M.M. Li, Q.W. Zhang, Y. Dai, Y.L. Li, X.Q. Zhang, Antiviral benzofurans from *Eupatorium chinense*, Phytochemistry 122 (2016) 238–245.
[16] F. Cullmann, K.P. Adam, H. Becker, Bisbibenzyls and lignans from *Pellia epiphylla*, Phytochemistry 34 (3) (1993) 831–834.
[17] A. Neudorffer, B. Deguin, C. Hamel, M.B. Fleury, M. Largeron, Electrochemical oxidative coupling of 4-hydroxycinnamic ester derivatives: a convenient methodology for the biomimetic synthesis of lignin precursors, Collect. Czechoslov. Chem. Commun. 68 (2003) 1515–1530.
[18] Y.M. Ren, C.Q. Ke, A. Mándi, T. Kurtán, C. Tang, S. Yao, Y. Ye, Two new lignan-iridoid glucoside diesters from the leaves of *Vaccinium bracteatum* and their relative and absolute configuration determination by DFT NMR and TDDFT-ECD calculation, Tetrahedron 73 (2017) 3213–3219.
[19] T.H. Kim, Hideyuki Ito, K. Hayashi, T. Hasegawa, T. Machiguchi, T. Yoshida, Aromatic constituents from the heartwood of Santalum alb*um* L, Chem. Pharm. Bull. 53 (2005) 641–644.
[20] J.J. Chen, T.Y. Wang, T.L. Hwang, Neolignans, a coumarinolignan, lignan derivatives, and a chromene: anti-inflammatory constituents from *Zanthoxylum avicennae*, J. Nat. Prod. 71 (2008) 212–217.
[21] J. Jin, C. Zhang, M. Zhang, Study on chemical constituents from *Aster tataricus* L.F, Modem Chin. Med. 10 (2008) 20–22.
[22] O. Spring, D. Vargas, N.H. Fischer, Sesquiterpene lactones and benzofurans in glandular trichomes of three *Pappobolus* species, Phytochemistry 30 (1991) 1861–1867.
[23] H. Li, S.Y. Peng, D.P. Yang, B. Bai, L.P. Zhu, C.Y. Mu, Y.J. Tian, D.M. Wang, Z.M. Zhao, Enantiomeric neolignans and a sesquiterpene from *Solanum erianthum* and their absolute configuration assignment, Chirality 28 (2016) 259–263.
[24] Y.C. Li, Y.H. Kuo, Four new compounds, ficusal, ficusesquilignan A, B, and ficusolide diacetate from the heartwood of *Ficus microcarpa*, Chem. Pharm. Bull. 32 (2010) 1862–1865.
[25] M. Haruna, T. Koube, K. Ito, H. Murata, Balanophonin, a new neo-lignan from Balanophora japonica Makino, Chern. Pharm. Bull. 30 (1982) 1525–1527.
[26] F. Cutillo, B. D'Abrosca, M.D. Greca, A. Fiorentino, A. Zarrelli, Lignans and neolignans from *Brassica fruticulosa*: effects on seed germination and plant growth, J. Agric. Food Chem. 51 (2003) 6165–6172.

[27] H. Jiang, L. Yang, G.X. Ma, X.D. Xing, M.L. Yan, Y.Y. Zhang, Q.H. Wang, B.Y. Yang, H.X. Kuang, X.D. Xu, New phenylpropanoid derivatives from the fruits of *Xanthium sibiricum* and their anti-inflammatory activity, Fitoterapia 117 (2017) 11–15.
[28] T.S. Wu, J.H. Yeh, P.L. Wu, The heartwood constituents of *Tetradium glabrifolium*, Phytochemistry 40 (1995) 121–124.
[29] Y.X. Zhao, X.D. Luo, J. Zhou, Lignans from *Tsuga dumosa*, Acta Bot. Yunnanica 26 (2004) 229–233.
[30] L. Xiong, C. Zhu, Y. Li, Y. Tian, S. Lin, S. Yuan, J. Hu, Q. Hou, N. Chen, Y. Yang, Lignans and neolignans from *Sinocalamus affinis* and their absolute configurations, J. Nat. Prod. 74 (2011) 1188–1200.
[31] O.V. Bryanskii, V.V. Tolstikhina, A.A. Semenov, A glycoside of syringaresinol from a tissue culture of *Scorsonera hispanica*, Chem. Nat. Compd. 28 (1992) 519–520.
[32] L.L. Landucci, S.A. Ralph, K.E. Hammel, 13C NMR characterization of Guaiacyl, Guaiacyl/Syringyland Syringyl dehydrogenation polymers, Holzforschung 58 (1998) 160–170.
[33] C.L. Zhang, Y. Wang, Y.F. Liu, D. Liang, Z.Y. Hao, H. Luo, R.Y. Chen, D.Q. Yu, Lignans from the rhizomes of Iris tectorum, Fitoterapia 108 (2016) 93–97.
[34] Y.L. Cui, M.U. Qing, C.Q. Hu, Syudies on the phenylpropanoids from *Caragana rosea*, Nat. Prod. Res. Dev. 27 (2003) 38–40.
[35] P. J. Houghton, Lignans and neolignans from *Buddleja davidii*, Phytochemistry 24 (1985) 819–826.